

Removal of Congo Red Dye Using Polyvinylidene Fluoride Polymer in Application Ultrafiltration Membranes

Mohammed M. Hassan^{1*} , Zaidun N. Abudi² , Mustafa H. Al-Furajji³ , Rouhollah Y. Farsani⁴ 

^{1,2} Environmental Engineering Department, College of Engineering, Mustansiriyah University, Baghdad, Iraq

³ Environment and Water Directorate, Ministry of Science and Technology, Baghdad, Iraq

⁴ Energy and Environment Research Center, Shahrekord Branch, Islamic Azad University, Shahrekord, Iran

*Email: ecma002@uomustansiriyah.edu.iq

Article Info	Abstract
<p>Received 18/07/2023</p> <p>Revised 26/03/2025</p> <p>Accepted 20/05/2025</p>	<p>The three ultrafiltration membranes prepared from different concentrations (13, 15, and 17 wt.%) of Polyvinylidene fluoride polymer are used to remove Congo Red Dye. The phase inversion method is utilized to fabricate the membranes. Membrane characterizations were studied using atomic force microscopy (AFM) to examine roughness. Scanning electron microscopy (SEM) was used to compare morphology and cross-sectional structure. Energy-dispersive spectrometry (EDS) determines the number, type, and distribution of atoms. Results showed that increasing the polymer concentration to 17 wt.% enhanced the membrane's hydrophobicity and improved dye rejection, attributed to higher surface roughness, a uniform and dense distribution of chemical elements (higher F and C peaks), and reduced porosity. Membrane performance was studied under operating pressures (2-7 bar) using a 100 ppm Congo Red dye solution in a cross-flow filtration system. The PVDF 17 wt.% membrane showed a flux rate of 4.46–41.89 L/m²·h at 2 and 7 bar, respectively, with 99% dye removal at 2 bar, decreasing to 94% at 7 bar.</p>

Keywords: Congo Red dye removal; Phase Inversion; Pressures; Ultrafiltration membrane; Water Flux

1. Introduction

One of the most effective ways to address the shortage of clean water supplies is to reuse water and wastewater by utilizing advanced treatment technology for both national and industrial needs [1]. The widespread discharge of sewage containing various dye species poses a threat to both people and the environment [2]. Massive wastewater unloading, which includes many dyes, is hazardous to the environment and poses a risk to human health [3]. It is known that the most popular azo dye, Congo red (CR), catabolizes the carcinogenic compound benzidine [4]. The dye can produce allergic reactions when exposed to it. Congo red has also been widely employed in the dye industry due to its low cost and superior adhesive properties [5]. However, the azo dye is frequently dumped into neighboring natural water streams as industrial wastewater, endangering the ecology. Therefore, it must be removed from wastewater [6].

As a result, several techniques, including biodegradation, extraction, electrophoresis, coagulation, photocatalysis, oxidation, and adsorption, were employed to treat wastewater containing the dye [5], [6]. However, it is essential to

acknowledge that the methods mentioned above have significant drawbacks, including the inefficiency of diluted solutions, the production of by-product sludge, and the need for post-treatment. One of the potential approaches for removing dyes from wastewater has been demonstrated to be membrane technology [3], [7]. Membrane technology has several advantages, including reduced operating costs, decreased energy consumption, a small footprint, a need for fewer chemical additives to remove pollutants, enhanced manufacturing efficiency, and quality control [8], [9]. Reverse osmosis (RO), microfiltration (MF), ultrafiltration (UF), and nanofiltration (NF) are a few of the membrane separation technologies used to treat water. A considerable amount of research has been conducted to determine the feasibility of using ultrafiltration (UF) membranes for wastewater treatment in the textile and leather tanning industries. Previous studies have shown that the UF method may retain numerous dye types, including methylene blue, safranin T, and crystal violet [10]. Using membrane technologies to recover dyes and other chemical elements from natural textile and leather tanning waste fluids successfully would be a more critical possibility at present. For the phase inversion method of manufacturing

ultrafiltration (UF) membranes, a significant range of synthetic polymer materials is commercially accessible. Among all these polymers, poly (vinylidene fluoride) (PVDF) is a semicrystalline polymer that has a wide range of uses due to its superior mechanical strength, chemical resistance, and thermal stability [10], [11].

This research aims to develop a research project to investigate the impact of preparation factors (such as porosity and polymer concentration) on UF membranes in terms of Congo Red Dye removal. For this purpose, the phase inversion technique fabricated pristine membranes of polyvinylidene fluoride (PVDF) with concentrations (13, 15, and 17 wt.%). SEM, EDX, AFM, and porosity were employed to investigate and characterize the membranes' hydrophobicity, cross-sectional morphology, and surface area roughness. The water permeability measurements and separation performance of dye removal from aqueous solution were also carried out under different pressures (2-7 bars). In comparison, the study's results differed from those of other studies [12]-[15], as evidenced by the following points: (1) different polymer concentrations that were accessible and useful were chosen, resulting in membranes having nanoporous structures with porosity and permeability acceptable, and (2) the results also demonstrated a high removal of dye. To the best of our knowledge, this is the first study to use a PVDF-UF membrane for removing Congo Red and dye under these operating conditions.

2. Materials and Experimental Works

2.1. Materials

The membrane material of Polyvinylidene fluoride (PVDF, $M_w = 534,000 \text{ g mol}^{-1}$, Sigma-Aldrich, USA) used in this work, NN-Dimethylformamide (DMF, $\text{H.CO.N (CH}_3)_2$, $M.W = 73.10 \text{ g mol}^{-1}$, Ambernath 421 501, India) was the polymer solvent, and Congo Red Dye [C.I. = 22120, chemical formula = $\text{C}_{32}\text{H}_{22}\text{N}_6\text{Na}_2\text{O}_6\text{S}_2$, $M.W = 696.7 \text{ g mol}^{-1}$, BDH Chemicals Ltd Poole England, UK]. All materials were purchased through a local dealer in Iraq and used without further purification.

2.2. PVDF Membranes Preparation

The membranes were prepared via the phase inversion method. The PVDF was dissolved at 60°C in the solvent DMF (a suitable solvent for PVDF) at three different concentrations (13, 15, and 17 wt.%). The solution was magnetically stirred for at least 8 hours to ensure thorough dissolution of the polymer. A hand-casting knife with a thickness of $180 \mu\text{m}$ casts the solutions uniformly onto a glass substrate and then submerges them into a coagulation bath at room temperature. The membranes were placed in a deionized water bath after complete coagulation and left for at least 24 hours to remove solvent remnants. Table 1 shows the composition of all membranes in the casting solution.

Table 1. Casting solution membranes

Type of Membranes	PVDF polymer (Wt. %)	DMF (Wt. %)
PVDF 13%	13	87
PVDF 15%	15	85
PVDF 17%	17	83

2.3. Performance of the Membranes Test

The performance of the membrane samples was evaluated based on their permeability and dye rejection characteristics. The PVDF UF membranes' water flux and rejection efficiency were assessed using a flat membrane module with an active area of (21 cm^2) . Fig. 1 depicts the UF configuration as a system. The preparing membrane was tested by the condition of passing 100 ppm of aqueous solutions for Congo Red dye at feed pressures at a range (2 -7 bars), (1) was used to determine the pure water flux of the samples for applying transmembrane pressures at room temperature.

$$F = \frac{V}{A \times \Delta t} \quad (1)$$

Where F ($\text{L/m}^2 \text{ h}$) is the water flux, A (m^2) is the effective membrane area, Δt (h) is the time taken for permeate collection, and V (L) is the volume of permeate.

The rejection efficiency (%) of the PVDF membrane was estimated by determining the concentration of dye in the feed (C_f) and permeate (C_p) flows (mg/L), respectively, as shown in equation (2).

$$R = \left(1 - \frac{C_p}{C_f} \right) \times 100 \quad (2)$$

Herein, C_p and C_f were determined by UV-Vis spectrophotometry.

2.4. Membrane Characterization Techniques

The surface and cross-sectional morphology of the membranes were examined using scanning electron microscopy (SEM) (FESEM Tescan Mira3, France) to determine the membranes that had formed. The membranes were ruptured and submerged in liquid nitrogen for 20 seconds for cross-sectional observation. The membranes were then wrapped in golden film. Finally, the SEM apparatus was used to evaluate the samples at an accelerating voltage of 20 kV. EDS was used to track and describe the components in the membranes. Atomic Force Microscopy (AFM) was used to examine the surface roughness of the manufactured membranes (Angstrom Advanced Inc., 2008, USA).

2.5. Porosity

The porosity of membrane samples was determined using a gravimetric technique. (W_w) stands for the wet weight (g) of the membrane area (6 cm^2), which is weighed first. The sample was dried for 24 hours. Before being reweighed to get its W_d represents dry weight (g), and the water density is (0.998 g/cm^3 at 25°C).

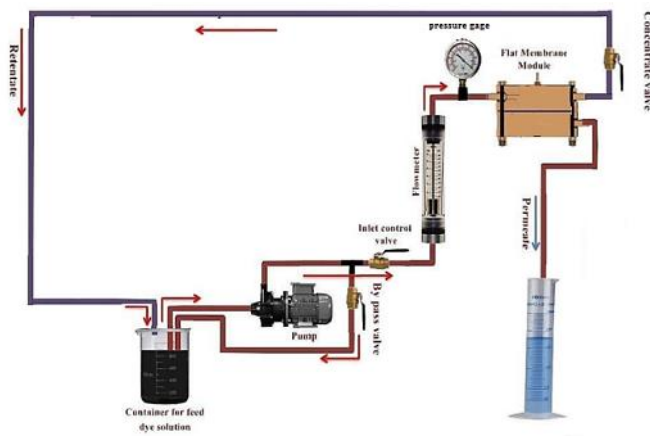


Figure 1. Diagram of UF membrane filtration process

The membrane sample's total porosity, ε (%), was determined using (3).

$$\varepsilon = \frac{Ww - Wd}{A \times t \times \rho} \quad (3)$$

The water density, effective membrane area, and membrane thickness are represented as ρ (g/cm^3), A (cm^2), and t (cm), respectively.

3. Results and Discussion

3.1. Membrane Characterization

3.1.1. Scanning electron microscopy test (SEM)

Fig. 2 displayed the impact of PVDF concentration on the membrane morphology. Throughout the phase inversion process, the composition constantly changes in response to the varying polymer and solvent concentrations in the casting solution. When the concentration of the solution increases, the number of lows and highs on the membrane surface increases, but their depth decreases [12], [14]. All PVDF membranes are characterized by nodules that vary in size and compactness. The selective layer's increased membrane skin thickness, resulting from a rise in concentration, substantially impacts the inner membrane structure. The cross-sectional images of the ultrafiltration PVDF 17 wt.% membrane show a dense and compact surface with no visible micropores that can be identified. Darvishmanesh et al. [16] found that as the concentration of casting polymer increases, the number of pores and microvoids decreases. Moreover, they discovered that as the polymer concentration increases, the membrane film thickness also increases, resulting in a decrease in membrane flux rates.

In contrast, the surface of the PVDF 13 wt.% and 15 wt.% membranes began to show an increasing number of wrinkles and micro-pores. Along the surface of membranes, the granular particle boundaries are linear and occasionally burst the surface. The pores in the membrane are formed by forming gaps between the granular objects, and their size and distribution are highly dependent on the overall porosity of the membrane [16], [17]. Because the size of these particles primarily determines the porosity of a membrane, it is expected that a membrane

prepared with a low polymer concentration will have greater porosity than a membrane prepared with a higher polymer concentration. In the case of the sponge part, as the macro voids' part shortens, it will become slightly larger [18].

Notably, the PVDF 17 wt.% membrane showed that an increase in polymer content causes porosity to decrease rapidly, which aligns with the findings of the Mulder study [19]. Additionally, Zhang et al. [17] demonstrated that the membrane pore size and porosity decrease rapidly as the casting polymer concentration increases. As a result, the dye's rejection ratio rises.

Surface SEM images

Cross-Sectional images.

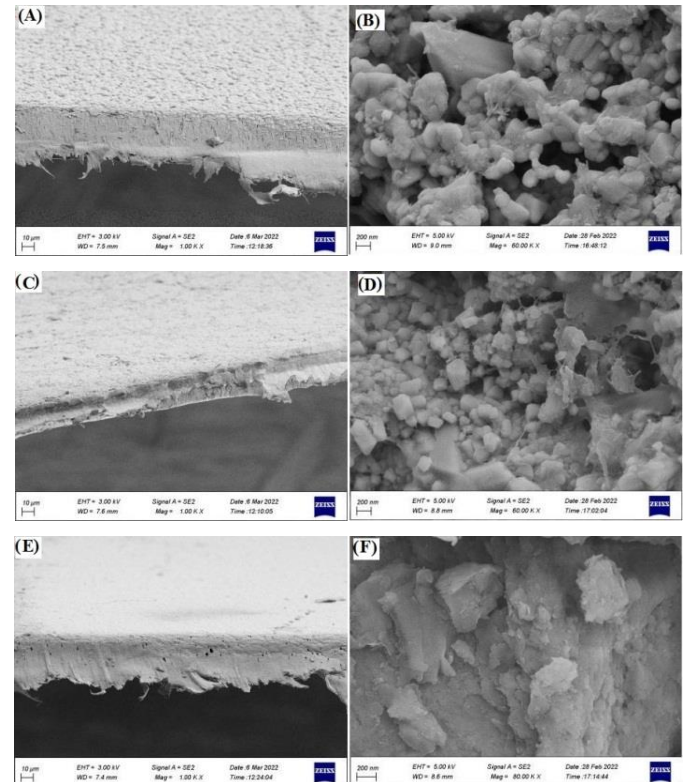


Figure 2. Surface SEM images of PVDF 13% (A), PVDF 15% (C), and PVDF 17% (E); cross-sectional SEM images of PVDF 13% (B), PVDF 15% (D) and PVDF 17% (F).

3.1.2. Energy dispersion spectrometry (EDS)

Energy-dispersive X-ray spectroscopy (EDS) was used to investigate the chemical composition of the produced membranes, revealing the distribution of atoms within the membranes and estimating the relative quantities of each atom. Fig. 3 shows the type and amount of each constituent for all forms of PVDF membranes. The characteristic peaks for elements O and F are observed in the EDS spectrum of membranes. The peaks for the elements Mg and Al partially overlap with those for Na or Zn. The faint peaks in the EDS spectra of the membrane's constituents may be caused by the shallow penetration depth used in EDS characterization techniques. In the spectra of the PVDF 13 wt.% membrane, no carbon peak was detected, and the fluorine peak was lowered.

In contrast, the oxygen peak recorded the highest ratio, which may interact with other molecules (such as water and epoxies) through van der Waals forces and hydrogen bonds on the polymer backbones. The hydrophilicity of the membrane surface was improved [20]. As a result, the permeability rate increases. This is due to the low concentration of the PVDF. Increasing the PVDF concentration in the membrane to 15 wt.% increased the F element content, a decrease in the O element content, and the appearance of the C element. On the other hand, the PVDF 17 wt.% membrane exhibited the highest F and C peaks and the lowest O peaks among the different membranes. Moreover, the high presence of C and F elements and the uniform dispersion of Mg, Ca, Na, and Si elements across the surface of the PVDF 17 wt.% membrane due to the PVDF support was identical to what is shown in the SEM images in Fig. 2. This observation means that this membrane showed a superhydrophobic surface and thus had a high dye rejection.

3.1.3. Atomic force microscopy (AFM) test

As shown in Fig. 4, three-dimensional (3D) and two-dimensional (2D) AFM surface images for all PVDF membranes are displayed in a scan area of $0.39 \times 0.39 \mu\text{m}$. It's also worth noting that the surface of the membrane exhibited valley and hill structures with different roughness for each type of formed layer. The brightest areas in these images represent the membrane's highest points, whereas the darkest areas denote valleys or membrane pores [21]. The membrane's roughness can be estimated by measuring the distance between its peaks and valleys, and there is a direct connection between a membrane's performance and roughness [22]. The PVDF 13 wt.% membrane showed lower roughness compared with the membrane of 15 wt.% of PVDF. However, increasing the concentration of PVDF to 17 wt.% displayed the highest roughness. Increasing the roughness would result in a decrease in water flux while the dye removal increases. According to Khayet et al. [23], the polymer concentration significantly impacts the membrane's porosity and roughness. They noticed that the surface roughness of the resultant membrane rises with an increase in PVDF solution concentration.

Additionally, they found that as the polymer concentration increased, permeability decreased, and retention increased. They concluded that the membrane's pore size and porosity are significant factors in these results. Tiraferri et al. [24] confirmed that as the casting polymer content increases from 9 to 18 wt.%, the water flux decreases, which is related to declines in membrane porosity and the number of microvoids.

3.1.4. Porosity

Membrane porosity is directly related to membrane morphology. All the membranes made from different concentrations of PVDF exhibited varying porosity, which is consistent with the SEM images shown in Fig. 2. The overall porosity of the membranes decreased as the concentration of PVDF polymer increased, as seen in Table 2.

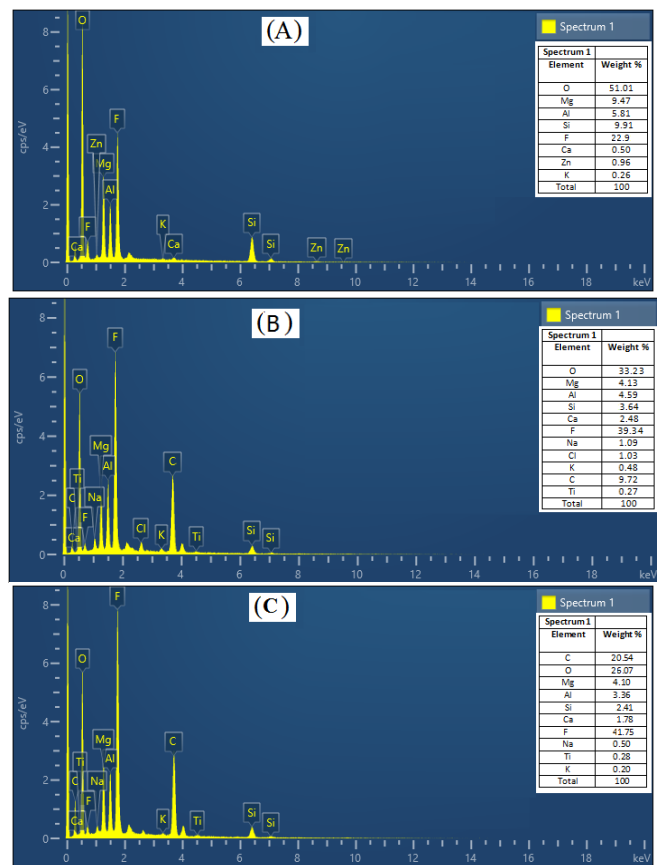


Figure 3. EDS analysis for PVDF 13% (A), PVDF 15% (B), and PVDF 17% (C) membranes.

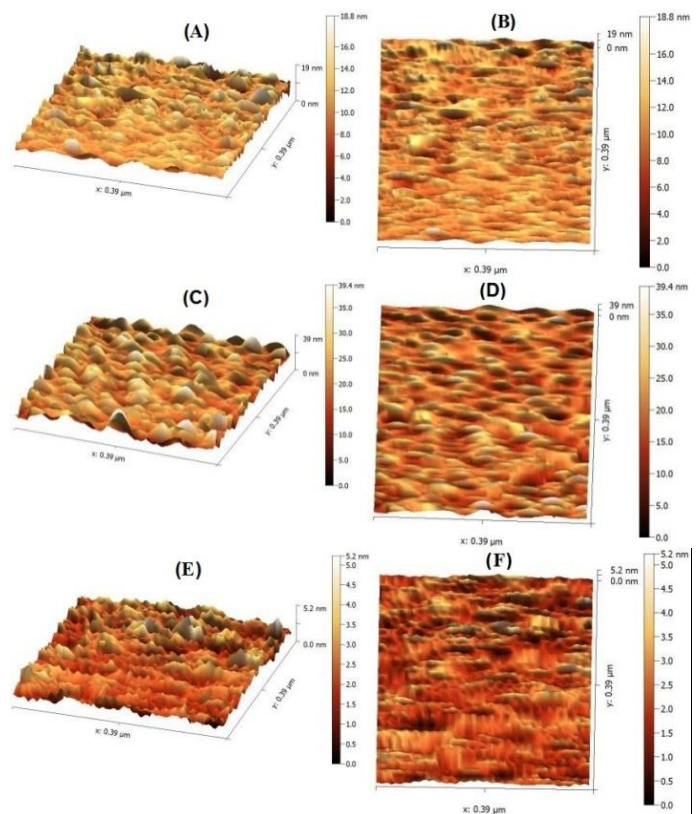


Figure 4. The 3D (left) and 2D (right) AFM images of PVDF 13% (A, B), PVDF 15% (C, D), and PVDF 17% (E, F).

Table 2. The surface roughness and porosity of PVDF membranes

Name of Surface Roughness	Porosity (%)	Surface Roughness, Ra (nm)
PVDF 13%	63	11
PVDF 15%	55	28
PVDF 17%	48	44

The resulting membrane from 13 wt.% PVDF presented a higher porosity of 63%, which further decreased with the addition of 15 wt.% PVDF, reaching a value of 55%. However, PVDF content of 17 wt.% caused a reduction in porosity at 48%. On the contrary, the surface roughness of the PVDF 17 wt.% membrane was higher than that of the other PVDF membranes. It is evident that concentration significantly alters the morphologies and porosities of membrane surfaces [25]. As concentration rises, the roughness criteria for membranes also rise. The pore size typically decreases as the surface roughness increases. Thus, membrane surfaces naturally show a distinct peak and valley. Generally, the granular item size decreases with increasing polymer concentration, resulting in a reduction in membrane porosity. Therefore, the concentration has a significant effect on membrane roughness [21].

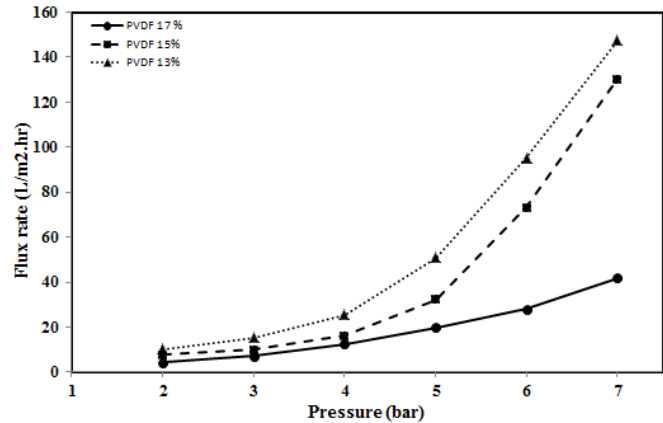
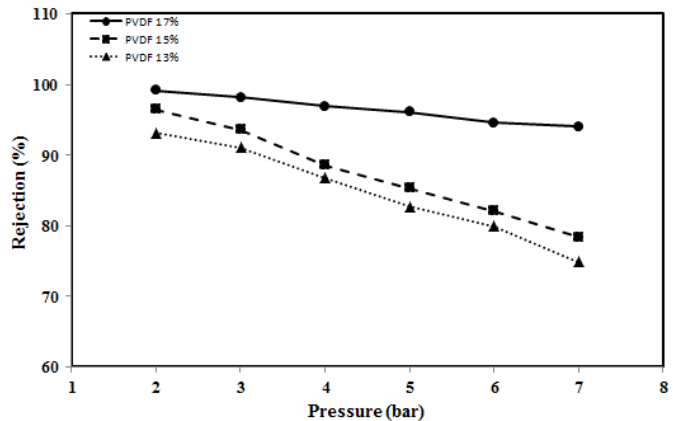
3.2. Permeability and rejection of dye versus operating pressure

The performance of each PVDF membrane was evaluated by measuring the flux rate and rejection of Congo Red dye at varying operating pressures. Fig. 5 and Fig. 6 show the water flux and dye rejection results for each type of polymer.

The pure water flux versus operating pressure for the three membranes is shown in Fig. 5. Observe that the PVDF 13 wt.% membrane had the highest water fluxes at 147.4 L/m² h at 7 bars. Otherwise, the average value of water flux found in the PVDF membrane is 15 wt.%. Regarding the PVDF, 17 wt.% membranes had the lowest value for the flow of water in the range (4.46 - 41.89) L/m² h in 2 and 7 bars, according to the test findings, respectively. These rates are considered acceptable despite the high rejection rates of dye for this membrane. By increasing the transmembrane pressure (TMP), the pure water flux of the membrane samples rises. This impact is linked to the increase in membrane driving force as transmembrane pressure rises. In other words, raising TMP increases the mass transfer driving force for water to pass through the membrane pores. While the membrane resistance remains constant, the pure water flux rises [26].

Fig. 6 shows the dye removal at different operational pressures. The highest dye removal was observed at 2 bar, with an efficiency of approximately 94% for the three membranes. The PVDF 17 wt.% was the optimal membrane, with removal percentages of 99% at 2 bar and 94% at 7 bar, as evidenced by the SEM test, indicating that the polymer layer was precisely produced. Conversely, dye removal at 7 bars decreased to approximately 70%, especially for the PVDF membranes with

13 and 15 wt.% concentrations. However, colossal pressure may reduce dye rejection due to increased concentration polarization [27]. The operating conditions usually determine the performance of a membrane in a practical application. As a result, it's critical to investigate membrane flux under various experimental conditions, such as operating pressure, operating time, and dye concentration [28]. Because dye rejections are declining, this study's findings indicate that pressure has a substantial impact on dye rejection.

**Figure 5.** Permeability as a function of operating pressure**Figure 6.** Dye rejection as a function of operating pressure

4. Conclusions

This research describes how ultrafiltration membranes were formed by utilizing Polyvinylidene fluoride (PVDF) polymer with varying concentrations (13, 15, and 17 wt.%) through phase inversion.

The SEM images demonstrated a shift in ultrafiltration membrane shape from porous to dense with increasing PVDF concentration to 17 wt.%.

According to the AFM test, the membranes with 13 and 15 wt.% of PVDF showed the least roughness compared to the PVDF 17 wt.% membrane. The most effective membrane has the highest roughness.

Increasing the peaks of F and C elements in the PVDF 17 wt.% due to increasing the polymer concentration in the membrane, as shown in EDS analysis.

The porosity of membranes decreased with increasing polymer concentration. Consequently increasing the hydrophobicity of membranes.

The operating pressures affected permeability and removal, as higher pressures increased flux and decreased dye rejection. An operating pressure of 2 bar is considered the optimum.

The PVDF 13 wt.% membrane exhibited a high flux rate of 147.4 L/m²/h, but dye removal significantly declined to 70% at 7 bars.

The results revealed that the PVDF 17 wt.% membrane's permeability rate is 5 L/m²/h at 2 bar and 42 L/m²/h at 7 bar. It also recorded the highest dye removal, between 99% and 94%, at a range of 2 and 7 bar, respectively. This demonstrates the significant potential for treating the dye in wastewater with such an optimal membrane.

Acknowledgments

The authors would like to thank Mustansiriyah University (www.uomustansiriyah.edu.iq), Baghdad, Iraq, for its support in the present work, as well as the Ministry of Science and Technology in Baghdad, Iraq.

Conflict of interest

The authors declare that the publication of this article does not cause any conflict of interest.

Author Contribution Statement

Mohammed M. Hassan designed and carried out the work in collaboration with Mustafa H. Al-Furaiji. Al-Furaiji and Zaidun N. Abudi proposed this research and supervised the work. All authors contributed to the methodology, theory development, and result analysis.

References

- [1] H. M. Alayan, I. R. Hussain, F. H. Kamil, M. M. Aljumaily, and N. A. Hashim, "Proficiency of few-layered graphene oxide nanosheets as promising sorbents for dye pollution management," *J. Environ. Eng.*, vol. 146, no. 8, p. 04020090, Aug. 2020. [https://doi.org/10.1061/\(ASCE\)EE.1943-7870.0001774](https://doi.org/10.1061/(ASCE)EE.1943-7870.0001774)
- [2] M. M. Hassan et al., "Studying the performance of various polymeric ultrafiltration membranes in dye removal," *Desalination Water Treat.*, vol. 280, pp. 139–156, 2022. <https://doi.org/10.5004/dwt.2022.29076>
- [3] M. K. Alomar et al., "N, N-Diethylethanolammonium chloride-based DES-functionalized carbon nanotubes for arsenic removal from aqueous solution," *Desalination Water Treat.*, vol. 74, pp. 163–173, 2017. <https://doi.org/10.5004/dwt.2017.20602>
- [4] S. Ghorai, A. K. Sarkar, A. B. Panda, and S. Pal, "Effective removal of Congo red dye from aqueous solution using modified xanthan gum/silica hybrid nanocomposite as adsorbent," *Bioresour. Technol.*, vol. 144, pp. 485–491, 2013. <https://doi.org/10.1016/j.biortech.2013.06.108>
- [5] N. H. H. Hairom, A. W. Mohammad, and A. A. H. Kadhum, "Nanofiltration of hazardous Congo red dye: Performance and flux decline analysis," *J. Water Process Eng.*, vol. 4, pp. 99–106, 2014. <https://doi.org/10.1016/j.jwpe.2014.09.007>
- [6] C. Lavanya et al., "Environmental friendly and cost effective caramel for Congo red removal, high flux, and fouling resistance of polysulfone membranes," *Sep. Purif. Technol.*, vol. 211, pp. 348–358, 2019. <https://doi.org/10.1016/j.seppur.2018.10.012>
- [7] A. M. S. Jorge, K. K. Athira, M. B. Alves, R. L. Gardas, and J. F. B. Pereira, "Textile Dyes effluents: a Current Scenario and the Use of Aqueous Biphasic Systems for the Recovery of Dyes," *Journal of Water Process Engineering*, vol. 55, p. 104125, Oct. 2023, doi: <https://doi.org/10.1016/j.jwpe.2023.104125>.
- [8] [8]M. Premaratne, G. Nishshanka, V. Liyanaarachchi, P. Nimarshana, and T. U. Ariyadasa, "Bioremediation of Textile Dye Wastewater Using microalgae: Current Trends and Future Perspectives," *Journal of Chemical Technology & Biotechnology*, vol. 96, no. 12, pp. 3249–3258, Jul. 2021, doi: <https://doi.org/10.1002/jctb.6845>.
- [9] R. R. Abdullah et al., "Novel photocatalytic polyethersulfone ultrafiltration (UF) membrane reinforced with oxygen-deficient tungsten oxide (WO_{2.89}) for Congo red dye removal," *Chem. Eng. Res. Des.*, vol. 177, pp. 526–540, 2022. <https://doi.org/10.1016/j.cherd.2021.11.008>
- [10] W. K. Al-Musawy, M. H. Al-Furaiji, and Q. F. Alsalhy, "Synthesis and characterization of PVC-TFC hollow fibers for forward osmosis application," *J. Appl. Polym. Sci.*, vol. 138, no. 35, p. 50871, 2021. <https://doi.org/10.1002/app.50871>
- [11] S. M. Doke and G. D. Yadav, "Novelties of combustion synthesized titania ultrafiltration membrane in efficient removal of methylene blue dye from aqueous effluent," *Chemosphere*, vol. 117, pp. 760–765, 2014. <https://doi.org/10.1016/j.chemosphere.2014.09.027>
- [12] J. Huang et al., "Evaluation of micellar enhanced ultrafiltration for removing methylene blue and cadmium ion simultaneously with mixed surfactants," *Sep. Purif. Technol.*, vol. 125, pp. 83–89, 2014. <https://doi.org/10.1016/j.seppur.2014.01.043>
- [13] S. Mondal, H. Ouni, M. Dhahbi, and S. De, "Kinetic modeling for dye removal using polyelectrolyte enhanced ultrafiltration," *J. Hazard. Mater.*, vol. 229, pp. 381–389, 2012. <https://doi.org/10.1016/j.jhazmat.2012.06.007>
- [14] X. Li and X. Lu, "Morphology of polyvinylidene fluoride and its blend in thermally induced phase separation process," *J. Appl. Polym. Sci.*, vol. 101, no. 5, pp. 2944–2952, 2006. <https://doi.org/10.1002/app.23932>
- [15] M. G. Buonomenna et al., "Poly(vinylidene fluoride) membranes by phase inversion: The role the casting and coagulation conditions play in their morphology, crystalline structure and properties," *Eur. Polym. J.*, vol. 43, no. 4, pp. 1557–1572, 2007. <https://doi.org/10.1016/j.eurpolymj.2007.01.030>
- [16] S. Darvishmanesh et al., "Novel polyphenylsulfone membrane for potential use in solvent nanofiltration," *J. Membr. Sci.*, vol. 379, no. 1–2, pp. 60–68, 2011. <https://doi.org/10.1016/j.memsci.2011.05.045>
- [17] Z. Zhang et al., "Effect of zero shear viscosity of the casting solution on the morphology and permeability of polysulfone membrane prepared via the phase-inversion process," *Desalination*, vol. 260, no. 1–3, pp. 43–50, 2010. <https://doi.org/10.1016/j.desal.2010.04.062>
- [18] A. Akbari et al., "Influence of PVDF concentration on the morphology, surface roughness, crystalline structure, and filtration separation properties of semicrystalline phase inversion polymeric membranes," *Desalination Water Treat.*, vol. 46, no. 1–3, pp. 96–106, 2012. <https://doi.org/10.1080/19443994.2012.677408>
- [19] M. Mulder, *Basic Principles of Membrane Technology*, 2nd ed. Dordrecht, Netherlands: Springer, 1996.
- [20] C. Sun and X. Feng, "Enhancing the performance of PVDF membranes by hydrophilic surface modification via amine treatment," *Sep. Purif. Technol.*, vol. 185, pp. 94–102, 2017. <https://doi.org/10.1016/j.seppur.2017.05.030>
- [21] K. Boussu et al., "Roughness and hydrophobicity studies of nanofiltration membranes using different modes of AFM," *J. Colloid Interface Sci.*, vol. 286, no. 2, pp. 632–638, 2005. <https://doi.org/10.1016/j.jcis.2005.01.095>
- [22] M. M. Aljumaily et al., "Modification of poly(vinylidene fluoride-co-hexafluoropropylene) membranes with DES-functionalized carbon

- nanospheres for removal of methyl orange by membrane distillation,” *Water*, vol. 14, no. 9, p. 1396, 2022. <https://doi.org/10.3390/w14091396>
- [23] M. Khayet, C. Cojocaru, and M. García-Payo, “Experimental design and optimization of asymmetric flat-sheet membranes prepared for direct contact membrane distillation,” *J. Membr. Sci.*, vol. 351, no. 1–2, pp. 234–245, 2010. <https://doi.org/10.1016/j.memsci.2010.01.052>
- [24] A. Tiraferri et al., “Relating performance of thin-film composite forward osmosis membranes to support layer formation and structure,” *J. Membr. Sci.*, vol. 367, no. 1–2, pp. 340–352, 2011. <https://doi.org/10.1016/j.memsci.2010.11.014>
- [25] M. B. Abid, R. A. Wahab, M. A. Salam, I. A. Moujдин, and L. Gzara, “Desalination technologies, Membrane distillation, and electrospinning, an Overview,” *Heliyon*, vol. 9, no. 2, p. e12810, Feb. 2023, doi: <https://doi.org/10.1016/j.heliyon.2023.e12810>.
- [26] K. Liu, Razi Epsstein, S. Lin, J. Qu, and M. Sun, “Ion–Ion Selectivity of Synthetic Membranes with Confined Nanostructures,” *ACS Nano*, vol. 18, no. 33, pp. 21633–21650, Aug. 2024, doi: <https://doi.org/10.1021/acsnano.4c00540>.
- [27] R. Javeed Ganaie, S. Rafiq, and A. Sharma, “Recent Advances in Physico-chemical Methods for Removal of Dye from Wastewater,” *IOP Conference Series: Earth and Environmental Science*, vol. 1110, no. 1, p. 012040, Feb. 2023, doi: <https://doi.org/10.1088/1755-1315/1110/1/012040>.
- [28]]P. Karami, M. M. H. Mizan, C. Ammann, A. Taghipour, J. B. P. Soares, and M. Sadrzadeh, “Novel Lignosulfonated Polyester Membranes with Remarkable Permeability and Antifouling Characteristics,” *Journal of Membrane Science*, vol. 687, p. 122034, Dec. 2023, doi: <https://doi.org/10.1016/j.memsci.2023.122034>.